

Noise assisted transport in the Wannier-Stark system

Stephan Burkhardt¹, Matthias Kraft^{1,2}, Riccardo Mannella³
and Sandro Wimberger¹

¹ Institut für theoretische Physik, Universität Heidelberg, Philosophenweg 19, 69120 Heidelberg, Germany

² Blackett Laboratory, Imperial College London, South Kensington Campus, SW7 2AZ London, UK

³ Dipartimento di Fisica ‘E. Fermi’, Università di Pisa, Largo Pontecorvo 3, 56127 Pisa, Italy

Abstract. We investigated how the presence of an additional lattice potential, driven by a harmonic noise process, changes the transition rate from the ground band to the first excited band in a Wannier-Stark system. Alongside numerical simulations, we present two models that capture the essential features of the dynamics. The first model uses a noise-driven Landau-Zener approximation and describes the short time evolution of the full system very well. The second model assumes that the noise process’ correlation time is much larger than the internal timescale of the system, yet it allows for good estimates of the observed transition rates and gives a simple interpretation of the dynamics. One of the central results is that we obtain a way to control the interband transitions with the help of the second lattice. This could readily be realized in state-of-the-art experiments using either Bose-Einstein condensates or optical pulses in engineered potentials.

1. Introduction

During the last years, there have been enormous advances in the experimental control over Bose-Einstein condensates (BECs) in optical lattices. States can be prepared with a high degree of control [1] and the systems can be isolated from external perturbations for long timescales [2]. This fine control over the system allows to investigate quantum mechanical effects that were previously very difficult to observe in experiments. Among these effects are Bloch oscillations, Wannier-Stark ladders, and Landau-Zener tunneling [3–5]. Dynamics similar to the ones observed in dilute BECs can nowadays also be realized using purely optical means [6, 7].

These advances have also paved the way to studying transport properties of spatially [8–12] or temporally disordered systems [13]. Disorder is to some degree present in almost all naturally occurring systems; in particular it plays a large role in solid state systems. New effects caused by disorder, such as Anderson localization have therefore potential ramifications in a wide range of fields.

But systems influenced by noise are not only an interesting subject due to their omnipresence; a noise process can also allow to fine-tune the properties of the system, as, for example, observed in the effect of stochastic resonance [14]. The question naturally arises, whether a similar effect can be seen in an optical lattice system driven by a noise process.

While most investigations of noise-driven systems focus on white [15] or exponentially driven noise [16–20], we use a process known as harmonic noise in this work. This noise process exhibits a strongly peaked power spectrum, corresponding to an oscillatory behaviour. It therefore introduces a characteristic noise frequency and has been observed to facilitate tunneling processes if this frequency matches the characteristic frequency of the system [21, 22]. In stochastic dynamics, it is now understood that the escape between attractors takes place along well defined "paths" in phase space, which are typically analytic [18, 23–26]: it is the matching between these structures and the stochastic noise which facilitates the escape, a phenomenon observed also in transient dynamics [27].

The system we consider in this work consists of a static tilted optical lattice which is disturbed by a second, noise-driven lattice. In the absence of the noisy lattice, the system corresponds to the well-known Wannier-Stark problem [28]. This Wannier-Stark system will be used as a reference system throughout this work.

Previous work by Tayebirad *et al.* [29] reports results based on numerical simulations of our system. In this paper, we will investigate the effects of the parameters of the noise process more thoroughly and introduce two different models that indeed explain many facets of the behaviour of the noise-driven problem.

In section 2 we will introduce the system studied in this paper and discuss it in the context of non-interacting BECs in optical lattices. We then introduce two models that allow for an interpretation of the behaviour of the system in section 3. An extensive numerical study is then presented in section 4; these results are compared to the models presented in the previous section and we give an outlook on weakly interacting BECs. We close with a short conclusion of the results in section 5.

2. Noisy Wannier-Stark system

In dimensionless units the Hamiltonian studied in this work reads

$$\hat{H} = -\frac{1}{2}\partial_x^2 + V_0 [\cos(x) + \cos(\alpha[x - \phi(t)])] - F_0x, \quad (1)$$

where V_0 gives the potential depth of the lattice, F_0 is the Stark force, α is a real number[‡] and $\phi(t)$ is a so-called harmonic noise process (introduced below). For a conversion between our dimensionless units, SI-units and common experimental units (applied e.g. in [5, 29, 30]), see appendix Appendix B.

[‡] If this number α is irrational, the resulting system is quasi-periodic, similar to those used to study Anderson localization by Roati *et al.* [12].

In the absence of the second phase-shifted stochastic lattice, the Hamiltonian in (1) corresponds to the well known Wannier-Stark system [31, 32]. A quantum state $|\psi\rangle$, which is sufficiently localized in momentum space (i.e. much smaller than the Brillouin zone) and prepared in the ground band, undergoes Bloch oscillations with the period $T_B = 1/F_0$ and partially tunnels into the first excited band everytime it reaches the edge of the Brillouin zone (corresponding to an avoided crossing of the respective energy bands). The characteristic time scale and frequency of the system are thus the Bloch period T_B and Bloch frequency $\omega_B = 2\pi/T_B$ [31]. The second potential term renders the system stochastic (via the phase ϕ) and spatially disordered in the static case ($\phi = \text{const}$) if $\alpha \notin \mathbb{Q}$.

Possible experimental realizations of such systems are for example BECs in optical lattices [5, 12]. Similar Hamiltonians are for example used for precision measurements of forces acting on the atoms of the BEC [33]. If the BEC is either dilute enough and/or interactions are suppressed by tuning with the help of a Feshbach resonance, their behavior can be well described by a single particle Hamiltonian as the one in (1) (see, e.g., [5, 30, 34]). In order to better understand how the observed effects would manifest in BECs with non-vanishing interactions, we will also look at simulations using the Gross-Pitaevskii equation in section 4.2. There are also recent experiments using optical pulses in engineered potentials that realize similar Hamiltonians [6, 7].

Let us briefly summarize the most important properties of harmonic noise. Harmonic noise can be imagined as a damped harmonic oscillator driven by gaussian white noise. It is defined via the two coupled stochastic differential equations [21, 22]

$$\dot{\phi} = \mu \tag{2}$$

$$\dot{\mu} = -2\Gamma\mu - \omega_0^2\phi + \sqrt{4\Gamma T}\xi(t), \tag{3}$$

where Γ is the damping coefficient, ω_0 sets the characteristic frequency of the noise and T determines the noise strength. $\xi(t)$ represents gaussian white noise [35, 36]. The equilibrium distributions of the noise variables are of bivariate gaussian type with first and second moments given by [22, 35]

$$\langle\phi\rangle = 0, \quad \langle\mu\rangle = 0, \quad \langle\phi^2\rangle = \frac{T}{\omega_0^2} \quad \text{and} \quad \langle\mu^2\rangle = T. \tag{4}$$

Just as the damped harmonic oscillator, harmonic noise can be classified into two different regimes, $\omega_0 > \sqrt{2}\Gamma$ and $\omega_0 < \sqrt{2}\Gamma$. In this paper we will only consider the first case, where the noise shows oscillatory behaviour and its power spectrum has a clear peak at a frequency $\omega_1 = \sqrt{\omega_0^2 - 2\Gamma^2} \approx \omega_0$ for $\omega_0 \gg \Gamma$ [22, 29, 35].

While the work of Tayebirad *et al.* provided a first numerical investigation of this system and showed that the noise properties have an influence on the observed transport, it could not answer the question after the mechanism of this influence [29]. In order to provide an answer to this problem, we present two simple models that explain how the noise process acts on the wavefunction in different regimes. We then compare the predictions of the two models with a more systematic numerical study and find that they give a good agreement with, and provide an intuitive understanding of the relevant

dynamics. Finally, we also look at the stability of the observed effects against nonlinear interactions as they would, e.g., be present in a realization using BECs.

3. Simplified Models

3.1. ‘Noisy’ Landau-Zener model

It turned out that the incommensurability of the two lattices does not have a great effect on the survival probability [37] due to the time-dependent phase $\phi(t)$. We will thus set $\alpha = 1$ and present a two state model that allows us to approximate the system’s dynamics around the band edge. The Hamiltonian of (1) now reads,

$$\hat{H} = -\frac{1}{2}\partial_x^2 + V_0 [\cos(x) + \cos(x - \phi(t))] - F_0x. \quad (5)$$

The translational invariance (at fixed time) of this Hamiltonian can be recovered by applying the gauge transformation $\psi = e^{iF_0xt}\tilde{\psi}$ (changing the frame of reference from the lab system to the accelerated lattice frame) [5, 31]. This yields,

$$\hat{H} = \frac{1}{2}(\hat{p} + F_0t)^2 + V_0 [\cos(x) + \cos(x - \phi(t))], \quad (6)$$

where we identified $-i\partial_x$ as the momentum operator \hat{p} . It is instructive to express this Hamiltonian in the momentum basis, this gives

$$\hat{H} = \int_p dp \frac{1}{2} [(p + F_0t)^2 |p\rangle\langle p| + V_0 ((1 + e^{i\phi})|p\rangle\langle 1 + p| + (1 + e^{-i\phi})|1 + p\rangle\langle p|)], \quad (7)$$

from which it is clear that it only couples states with $\Delta p = p - p' \in \mathbb{Z}_0$ (due to the time evolution). The momentum states can thus be written as $|p\rangle = |n + k\rangle$, with $n \in \mathbb{Z}_0$ and $k \in [-0.5, 0.5) \subset \mathbb{R}$ being the quasimomentum of the system. Due to the conservation of quasimomentum, the Hamiltonian in (7) can be decomposed into independent Hamiltonians each acting on a subsystem of constant quasimomentum k [5, 38]. A system initially in state $|p_0\rangle = |k_0 + n\rangle$ thus evolves according to the (tridiagonal) matrix Hamiltonian,

$$\hat{H}_{k_0} = \frac{1}{2} \begin{pmatrix} \ddots & V_0(1 + e^{i\phi}) & & & \mathbf{0} \\ & (\mathbf{k}_0 - \mathbf{1} + \mathbf{F}_0\mathbf{t})^2 & \mathbf{V}_0(\mathbf{1} + \mathbf{e}^{i\phi}) & & \\ & \mathbf{V}_0(\mathbf{1} + \mathbf{e}^{-i\phi}) & (\mathbf{k}_0 + \mathbf{F}_0\mathbf{t})^2 & V_0(1 + e^{i\phi}) & \\ & & V_0(1 + e^{-i\phi}) & (k_0 + 1 + F_0t)^2 & \\ \mathbf{0} & & & V_0(1 + e^{-i\phi}) & \ddots \end{pmatrix}, \quad (8)$$

where the $V_0(1 + e^{\pm i\phi})$ terms stem from the optical lattices and ϕ enters as a complex phase. The dynamics of the full system around an avoided crossing of the ground and first excited energy band (at the edge of the Brillouin zone) can be approximated by the **highlighted** part of the above matrix[§] with $k_0 = 0.5$, i.e. the value at the edge of

[§] This corresponds to reducing the system to the two lowest energy states. At the edge of the Brillouin zone, this approximation is very accurate as long as the off-diagonal coupling terms are not too large, since only the lowest energy states contribute to the first excited as well as the ground band.

the Brillouin zone [5, 38]. This yields a reduced Hamiltonian

$$\hat{H}_{N,LZ} = \frac{1}{2} \begin{pmatrix} -F_0 t & V_0(1 + e^{i\phi}) \\ V_0(1 + e^{-i\phi}) & F_0 t \end{pmatrix}, \quad (9)$$

where we additionally subtracted $\frac{1}{4} + (F_0 t)^2$, i.e. we shifted the absolute value of the energy scale. This 2-by-2 matrix can be seen as an effective ‘noisy’ Landau-Zener (LZ) Hamiltonian; its *instantaneous* eigenvalues are given by,

$$E_{N;1,2} = \mp \frac{1}{2} \sqrt{(F_0 t)^2 + 2V_0^2(\cos(\phi(t)) + 1)}. \quad (10)$$

We can thus introduce an *effective band gap* as a function of time by averaging over the probability distribution of the noise process ϕ . At $t = 0$, this leads to

$$\Delta E_{\text{eff}} = V_0 \left[\langle \sqrt{2(\cos(\phi(0)) + 1)} \rangle \pm \text{Std} \left(\sqrt{2(\cos(\phi(0)) + 1)} \right) \right], \quad (11)$$

where $\langle f(\phi) \rangle$ denotes the average over the noise process and ‘Std’ means standard deviation (see figure 6 for a schematic representation of ΔE_{eff}).

In the case of a single (noiseless) optical lattice only the constant term in the anti-diagonal of the Hamiltonian in (9) is present and one recovers the standard LZ model [39–42]. Starting in the ground state at time $t = -\infty$, the probability to remain in that state until time $t = \infty$ is given by the Landau-Zener formula [39–42],

$$P_{\text{sur}}(t = \infty) = 1 - \exp \left(-\frac{\pi V_0^2}{2F_0} \right). \quad (12)$$

This allows to give estimates for the survival probability in the ‘noisy’ LZ model by replacing V_0^2 with ΔE_{eff}^2 in (12).

The two state approximation around an avoided crossing is only applicable if the initial momentum distribution is sufficiently localized in momentum space (i.e. much smaller than the Brillouin zone) [30] and if the characteristic time of the system is larger than the transition time in the two state model [43, 44], i.e. the transition time should be smaller than one *Bloch period*.

3.2. Quasistatic model

Since the noisy LZ model is limited to short timescales and can only be applied if both lattices in (1) have the same wavelength, we will present another model which is able to describe the behaviour of the system in cases where those conditions are not met.

This model is based on a quasistatic approximation of the noise process; $\phi(t)$ is replaced by a term βt linear in time. The resulting system is analyzed and its observables are averaged according to the properties of the noise process. In the following paragraphs, we will provide a more detailed description of this model.

For short timescales, the dynamics of the system can be approximated by a Taylor expansion of the noise term $\phi(t)$:

$$\phi(t + \epsilon) = \phi(t) + \epsilon \frac{d}{dt} \phi(t) + \text{O}(\epsilon^2) = \phi(t) + \epsilon \mu + \text{O}(\epsilon^2). \quad (13)$$

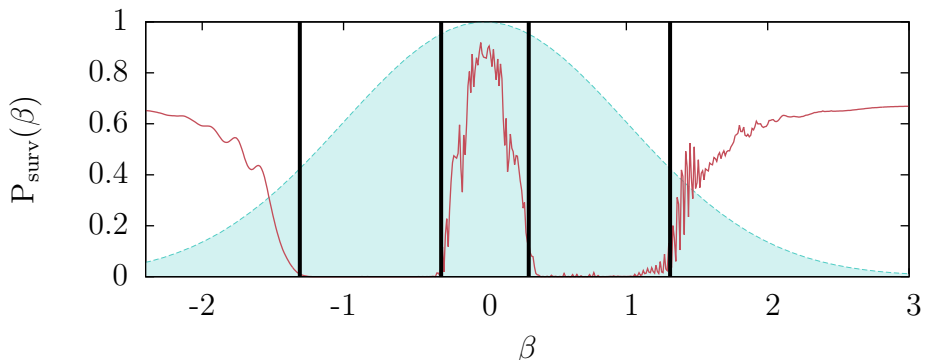


Figure 1: The fluctuating red curve shows the survival probability for the noiseless bichromatic lattice for a relative lattice velocity of β . The parameters are $\alpha = 0.61$, $F_0 = 0.00762$, $\Gamma = 0.00762$ and $V_0 = 0.125$. The black bars mark the values of β which lead to an intertwined position of the barriers (see figure 2). The blue gaussian curve of variance T gives the probability distribution of μ given in (4). In the quasistatic model, we set $\beta = \mu$ and $P_{\text{sur}}(\beta)$ is therefore averaged over this gaussian distribution.

A rigorous mathematical treatment of the ϵ^2 term in (13) is far from trivial^{||}. Nevertheless, it is clear that it depends on $\frac{d^2}{dt^2}\phi(t) = \frac{d}{dt}\mu(t)$ as given in (3) and is thus negligible for $\omega_0, \Gamma \ll 1$. In this case, (1) can therefore be approximated as

$$H = -\frac{1}{2}\partial_x^2 + V_0 \cos(x) + V_0 \cos(\alpha(x - \phi_0 - \beta t)) + Fx, \quad (14)$$

where the noise variable $\mu(t)$ has been replaced by a constant term β . Equation (14) describes a tilted bichromatic optical lattice system where the two lattices have a constant relative velocity β . The dynamics of such a system can be seen in figure 1. The fluctuating red curve shows the survival probability of the state in the ground band after $t = T_B$. It can be seen that this survival probability drops sharply for intermediate values of β ($|\beta| \approx 0.31 - 1.31$, region between the black vertical lines). This corresponds to strongly enhanced interband transport for these parameters.

As in section 3.1, the key to understanding lies in considering the effect of optical lattices on the wavefunction in momentum space. Let us first look at a single tilted optical lattice $V_0 \cos(\alpha x)$. We assume that the timescale of the Landau-Zener transition from the ground band to the first excited band is short compared to a Bloch period and is thus accurately described by the Landau-Zener model. Due to the static force F , a momentum-eigenstate scans through momentum space; once it reaches a momentum $p = \pm \frac{\alpha}{2}$, it undergoes a reflection on the lattice with the probability of P_{sur} given in (12). This process is schematically displayed in figure 2 (left). For the ground band, the effect of the lattice can therefore be represented as a pair of barriers at $\pm \frac{1}{2}\alpha$ (blue barriers in left of figure 2), which trap the state in between them. This momentum range between

^{||} As the second time derivative of the noise term $\phi(t)$ is not well-defined, it is necessary to look at a value $\langle \phi(t) \rangle$ which is averaged over a timescale, which is much shorter than the characteristic one of the system.

the barriers corresponds to the ground band. For the lattice moving with velocity β , the position of these barriers in momentum space is shifted to $(\pm\frac{\alpha}{2} + \beta)$. Adding up the effects of both, static and moving lattice thus results in the presence of two pairs of barriers as seen in the right part of figure 2. If the two pairs of barriers are in an intertwined position (as shown in the right of figure 2), reflections on the moving lattice can help the state escape from the ground band. This can be understood from the right part of figure 2. If the state ‘hits’ the barrier at $k = -\frac{\alpha}{2} + \beta$ from the left (green barriers in figure 2), it can either be transmitted or reflected. While the transmitted fraction of the state is still trapped in-between the barriers at $k = \pm\frac{\alpha}{2}$, the reflected fraction appears at the right side of the barrier at $k = \frac{\alpha}{2} + \beta$ and has thus escaped the ground band of the non-moving lattice. This can be interpreted as absorbing momentum from the moving lattice by means of a Bragg reflection and thus being ‘boosted’ out of the ground band. It should be noted that the same process can also take place for negative beta (transporting the state to the left of ground band in figure 2, therefore also out of the ground band). Transport to higher energy bands is therefore enhanced for intertwined barriers. This is supported by the data visible in figure 1, where the values of β which lead to an intertwined configuration are the area in-between the black vertical lines. These values of β do indeed correspond to a heavily suppressed survival probability in the ground band and thus to strongly enhanced transport.

Keeping this picture in mind, we can understand how the noise process acts upon the momentum states of the system. The constant β is responsible for the relative position of the barriers in momentum space. In the real system, β is given by the noise variable $\mu(t)$ and is thus a function of the time. The positions of the barriers of the noise driven lattice thus move in momentum space.

In our quasistatic model we assume $\mu(t)$ to be a constant β , which is a realistic approximation as long as the noise process is slow, i.e. $\mu(t)$ changes slowly with time. For $\mu(t) = \beta$ the survival probability in the ground band is given by figure 1. To obtain an approximation for the behavior of the full, noise-driven system, we thus average this survival probability $P(\beta)$ over the equilibrium distribution of $\mu(t)$, which is a gaussian of width T (see (4)) as pictured in figure 1.

While we would expect this model to be accurate for slow noise processes, it ignores

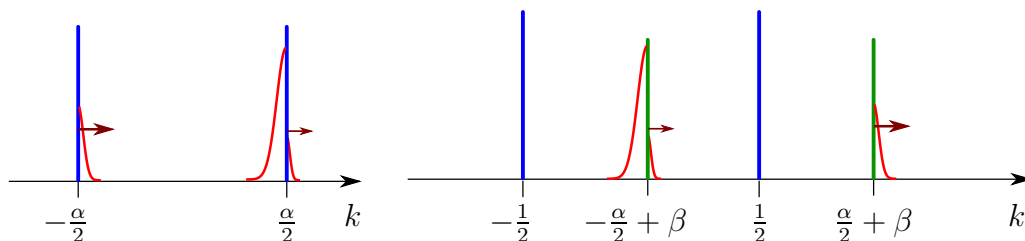


Figure 2: Left: Effect of a single lattice on momentum eigenstates. Right: Combined effect of a static and moving lattice.

the influence the non-static nature of $\mu(t)$ has on the Landau-Zener transitions and does also not account for time-correlations of the noise-process. Especially for a fast noise process where $\mu(t)$ changes significantly during one Bloch period, we therefore expect discrepancies between the quasistatic model and the full system [45].

4. Numerical Results

We compare now the predictions made by the two models introduced in the previous section with data from the full system described by the Hamiltonian in (1).

The most important property of the noise process ϕ is its *variance*. In the following, we will analyze the survival probability of the system in the ground band for the two cases: $\text{Var}(\phi) = \text{constant}$ (section 4.1) and $\text{Var}(\phi) = \text{changing}$ (section 4.2). The latter is realized by keeping ω_0 constant and varying T .

Figure 3 shows the survival probability in the ground band after one Bloch period. The survival probability strongly depends on the noise parameters T and ω_0 .

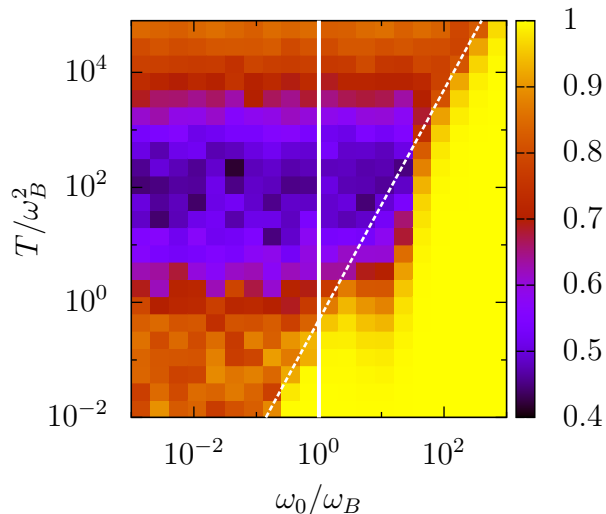


Figure 3: Survival probability of the system described by (1) in the ground band (colour coded) after $t = T_B$, i.e. after one transition, versus the rescaled noise frequency ω_0/ω_B and the noise strength T/ω_B^2 . The vertical solid line represents a line of constant ω_0 . The inclined dashed line represents a line of constant variance. Data from numerical simulations of the Hamiltonian in (5), for details see appendix Appendix A. The parameters are $F_0 = 0.00762$, $\Gamma = 0.00762$ and $V_0 = 0.125$.

4.1. Constant variance, i.e. $T/\omega_0^2 = \text{const}$.

Here, we show the survival probability in the ground band after one Bloch period for constant variance (cut along the dashed line in figure 3) versus the noise frequency. We focus on the region of the initial decrease and minimum of the survival probability, i.e. $\omega_0/\omega_B \lesssim 14$. Figure 4 compares numerical data from the ‘noisy’ LZ model in (9), with data from the full Hamiltonian in (5) for two values of the potential depth V_0 .

There is an excellent qualitative and a good quantitative agreement between the ‘noisy’ LZ predictions and the simulations of the full system. The ‘noisy’ LZ accurately reproduces the initial decay of the survival probability (as obtained for the stochastic Wannier-Stark system) for increasing noise frequency and gives a good approximation

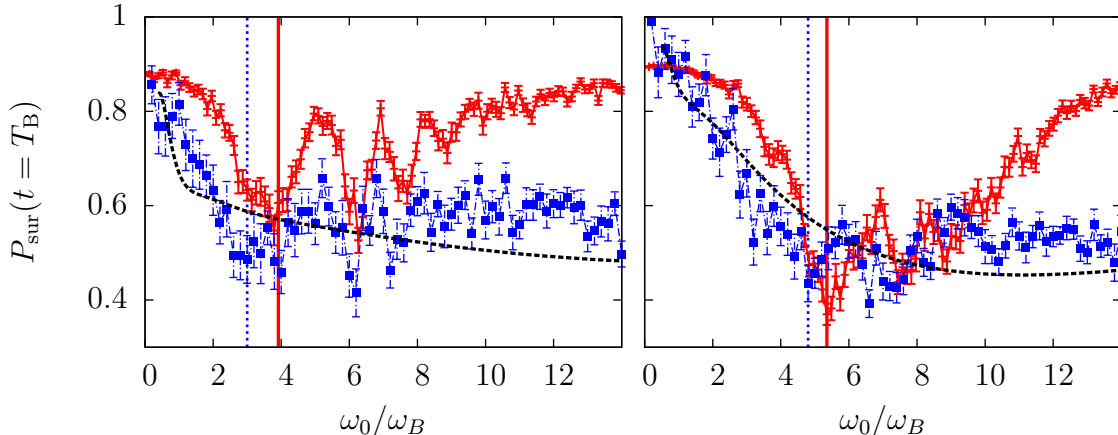


Figure 4: Survival probability in the ground band at $t = T_B$ versus the rescaled noise frequency ω_0/ω_B . Shown are data for the real system (blue dashed lines), the ‘noisy’ LZ model (red solid line) and the quasistatic model (black dotted line). The vertical lines indicate the position of the first minimum in the survival probability for their respective data sets. The parameters are $F_0 = 0.00762$, $\Gamma = 0.00762$, $\langle \phi^2 \rangle = 0.5$ and $V_0 = 0.0625$ (left) and $V_0 = 0.125$ (right).

for the position of the minimum. Yet, it systematically overestimates the survival probability. This overestimation is less pronounced for higher potential depths V_0 (compare figure 4 (left) and figure 4 (right)). Most importantly, the position of the minimum changes with varying potential depth V_0 . The quasi-static model also shows a decrease in the survival probability with increasing frequency, but cannot reproduce any of the finer features visible in the stochastic Wannier-Stark system and the ‘noisy’ LZ-model.

The varying position of the minimum leads us to the next figure, figure 5, in which the position of the first minimum in the survival probability is plotted versus the potential depth V_0 . Here, the predictions of the ‘noisy’ LZ model and the quasistatic model are compared to the full system; also the effective band gap ΔE_{eff} is plotted as a function of V_0 . The data for the full system shows that there exists a linear relationship between the position of the minimum in (4) and the potential depth V_0 . This relationship is accurately reproduced by the ‘noisy’ LZ model, but it can not be seen in the quasistatic model. The fact that the quasistatic model can not account for the position of the minimum is easily understood by looking at figure 4. Since the model does not predict the local minima visible in P_{sur} of both the full system as well as the noisy LZ model, it is clear that the position of the first minimum will in general be at much larger values of ω_0 .

Another observation that can be made in figure 5 is that the slope of the linear curve (for the full system and the LZ model) is approximately given by the one for the effective band gap. In fact, linear fits to the data give a slope of 1.93 for the real system and 1.76 for the LZ model, compared to 1.88 ± 0.15 for the effective band gap (11).

Hence, within errors, the position of the minimum is given by the effective band gap plus a constant off-set. The linear relationship also holds for different values of F_0 [37].

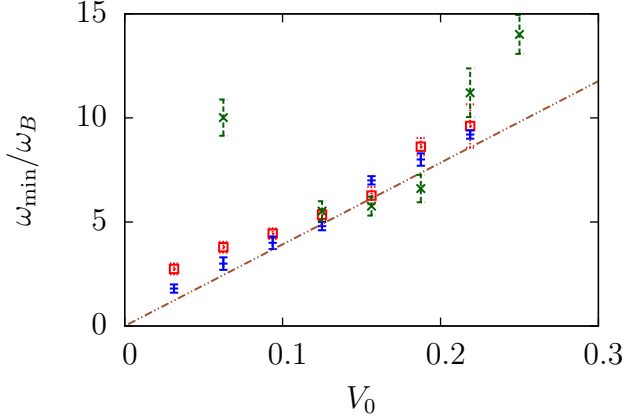


Figure 5: Frequency position of minimum versus potential depth V_0 . Shown are the data for the real system (blue lines), the ‘noisy’ LZ prediction (red squares), the quasistatic model prediction (green crosses) and the effective band gap ΔE_{eff} (dashed-dotted line). The parameters for the numerical simulations are $F_0 = 0.00762$, $\Gamma = 0.00762$, $\langle \phi^2 \rangle = 0.5$.

The linear dependence of the minimum on V_0 can be interpreted as follows. As mentioned in section 2, the harmonic noise ‘feeds’ an energy of $\approx \omega_0$ into the system. Once this energy is high enough to overcome the band gap between the ground and first excited band, given by $\approx \Delta E_{\text{eff}}$, the system can be excited into the upper band via a ‘phononic’ excitation process¶ (red wiggly lines in figure 6).

The overestimation of the survival probability by the ‘noisy’ LZ model occurs because the ‘LZ’ model overestimates the separation of the bands in the real system far away from an avoided crossing (the model only works in the blue shaded region of figure 6); hence transitions to higher bands are suppressed (the effective bandgap increases linearly with time t for large times, see figure 6). For large V_0 , only transitions close to an avoided crossing can occur, but for smaller V_0 transitions across the full Brillouin zone happen in the real system and this can not be ignored.

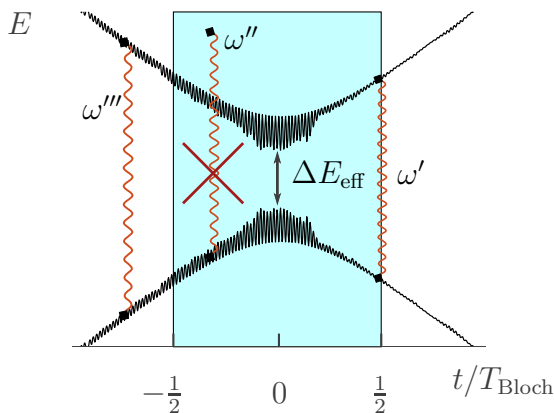


Figure 6: Instantaneous eigenvalues (solid black lines) of the ‘noisy’ LZ model for a typical noise realization. Schematically represented are ΔE_{eff} and transitions between energy states (red wiggly lines). The blue shaded area extends over one Bloch period and approximates the energy band structure of the ‘noisy’ WSS around an avoided crossing. The crossed out transition is not allowed.

¶ ‘Phononic’ is not to be taken literally, but indicates that the energy is transferred to the atoms via an optical lattice shaking/vibrating with a more or less well-defined frequency of $\approx \omega_0$.

The early rise of the survival probability in the ‘noisy’ LZ model is due to its two band nature. If the energy fed into the system by the noise is too large, there exists no target state for the transition (see crossed out transition in figure 6). In the real Wannier-Stark system, this rise happens only at higher ω_0 because it is not just a two band system and transitions to higher bands are actually possible.

4.2. Changing variance, i.e. constant ω_0 and varying T .

In figure 3 we observe the following: once ω_0 assumes a small enough value it stops having a discernible influence on the survival probability P_{sur} in the ground band. In this section we will therefore take a more detailed look at how P_{sur} in this regime depends on T while keeping $\omega_0 = 1$ constant.

On the left side of figure 7, we see the survival probability of a system initially prepared in the ground state in comparison to the predictions from the two models. The observable $P_{\text{sur}}(t = T_{\text{Bloch}})$ is the same as previously looked at in figure 4. Good qualitative agreement between the full system and both models is observed. Furthermore, within the numerical errors, the minimum of the survival probability is correctly predicted by both models. There are, however, quantitative discrepancies for small (noisy LZ model) as well as large values of T (quasistatic model).

On the right side of figure 7, a system with two different lattice constants is studied ($\alpha = 0.618$). The quantity analyzed in this case is the large time survival probability of the ground state per Bloch period $P_{\text{sur}}(t + T_{\text{Bloch}})/P_{\text{sur}}(t)$ for $t > 5$. This quantity is similar to the previously examined survival probability $P_{\text{sur}}(t = T_{\text{Bloch}})$, but it is

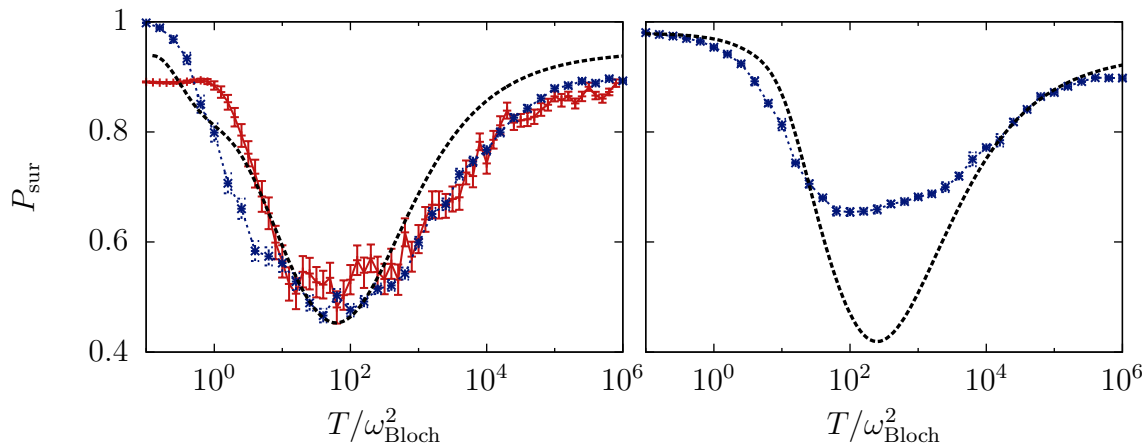


Figure 7: Survival probability in the ground band for fixed noise parameter ω_0 . Plotted are the results from the full system (blue stars), the predictions by the noisy LZ model (red line) as well as the predictions from the quasistatic model (black dashed line). Parameters are $F_0 = 0.00762$, $\Gamma = 0.00762$, $V_0 = 0.125$ and $\alpha = 1$ (left) and $\alpha = 0.618$. The plotted quantity is the survival probability after one Bloch period $P_{\text{sur}}(t = T_{\text{Bloch}})$ (left) and the average survival rate for long timescales $P_{\text{sur}}(t + T_{\text{Bloch}})/P_{\text{sur}}(t)$ (right).

derived from the long term exponential decay of the initial state. No results for the noisy LZ model are shown since this model cannot make any predictions for the case $\alpha \neq 1$. For the quasistatic model, good quantitative agreement with the full system is observed for most values of T . Nevertheless, significant differences are visible around the predicted minimum. These differences, however, result from the limitations of the quasistatic model and vanish if ω_0 as well as Γ are chosen small enough. In this case, where $\alpha \neq 1$, the quasistatic model is very successful in quantitatively predicting the long-term survival probabilities, especially if Γ as well as ω_0 are small [45].

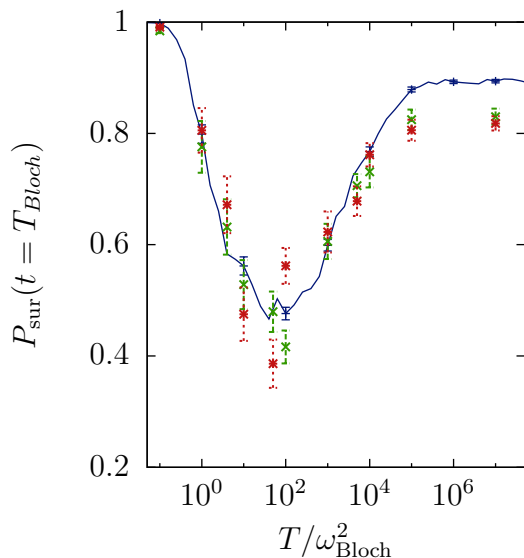


Figure 8: Survival probability in the ground band after one Bloch period using the Gross-Pitaevskii equation (same parameters as left of figure 7). Results from the (linear) Schrödinger equation are shown in solid blue, while green crosses show results for $N = 5 \cdot 10^4$ and red stars for $N = 10^5$ atoms in a cigar-shaped condensate. The simulated setup was the one used in the experiments reported in [46] and is described in Appendix A. The used atom numbers correspond to dimensionless nonlinearity parameters of $C \approx 0.08$ (green crosses) and $C \approx 0.13$ (blue stars), c.f. ref. [32, 46].

In order to understand whether the described effects would be visible in a realistic experimental setup using BECs, it is important to know how they are affected by interactions between the atoms in a condensate. Using the 3D Gross-Pitaevskii equation, we performed numerical calculations for an experimental setup similar to the one used in [46]: ^{87}Rb atoms that are placed in a cigar-shaped optical dipole trap with 250Hz radial and 20Hz longitudinal frequency. The results can be seen in figure 8 and show that, while clear differences in the survival probability exist, the enhanced tunneling rate for intermediate noise frequencies persists and is hardly influenced by the nonlinearity. It should especially be noted that for a nonlinearity parameter (as defined in [46]) up to $C \approx 0.13$, the position of the minimum is hardly changed from the single particle dynamics⁺.

⁺ Nonlinearity parameters are only given approximately, as they depend on the maximal density of the condensate. Since our setup is governed by a stochastic equation, the peak density of the condensate is not only time-dependent due to the interband tunneling [47], but also fluctuates for different noise realizations.

5. Conclusion

We have investigated the transport properties of a bichromatic Wannier Stark problem under the influence of harmonic noise. Our main interest was understanding the circumstances under which the noise process can enhance or suppress the transport in momentum space.

An extensive numerical study of the influence of the noise parameters revealed that the system's behaviour can be divided into two different regimes, as seen in figure 3. In the regime of low variance of the noise process, the noise only has very little influence, while in the regime of large variance, the properties of the system almost exclusively depend on the noise strength T . In this regime of large variance, the transport in momentum space has a clear maximum for a certain value of T .

We presented two different models that both offer an interpretation of these results. The noisy LZ model approaches the system as a noise-driven Landau-Zener transition and argues that transport should be maximized if the noise frequency matches the band gap between the ground and the first excited band. While this model can only predict results for the case where both lattices have the same wavelength, it reproduces the numerical results of the full system in this case very well. Furthermore, it gives an accurate prediction of the noise parameters necessary to maximize transport (see figure 5). The quasistatic model assumes the noise process to be slow compared to the timescales of the noise-free system. Linking the relative velocity of the optical lattices to their action upon the wavefunction in momentum space, this model predicts that the transport rate only depends on the noise parameter T and achieves a maximum for intermediate values of T . Within the low-variance regime seen in figure 3, this prediction matches very well with the results of the full system, even if full quantitative agreement is only reached for very slow noise processes. Our quasistatic model, where the particle is effectively kicked by the moving second lattice, see figure 2, may turn out to be relevant as well for the understanding of damping effects of Bloch oscillations in 'noisy' solid-state devices [48, 49].

Since experiments that study the expansion of the wavefunction in noise-driven lattices are underway [13], an experimental realization of our system and a comparison between experimental and numerical data would be interesting. As shown at the end of section 4.2, the observed effects are fairly stable against interactions between the atoms of a BEC and should therefore be easily observable. Besides possible realizations with BECs in optical lattices [12], purely optical techniques such as the one of [6] could also be used. While control over the BEC using a noise process is subject to large fluctuations, a deterministic bichromatic lattice, as presented in the beginning of section 3.2, could be used to control the transport between different bands with a high degree of precision. In figure 1 we, e.g., can see that with small changes of the relative lattice velocity β , the tunneling rates can be easily tuned by various orders of magnitude.

Acknowledgments

We thank Niels Lörch for help and discussions at an early stage of this work. Furthermore, we are grateful for the support of the Excellence Initiative through the Heidelberg Graduate School of Fundamental Physics (Grant No. GSC 129/1), the DFG FOR760, the Heidelberg Center for Quantum Dynamics and the Alliance Program of the Helmholtz Association (HA216/EMMI).

Appendix

Appendix A. Numerical methods

The data for the ‘noisy’ LZ model is obtained by numerically integrating the Schrödinger equation corresponding to Hamiltonian (9). The survival probability has been obtained by starting in the *adiabatic* ground state (i.e., in the momentum eigenbasis of the uncoupled problem [34]) at $t = -0.5T_B$ and then propagate it to $t = 0.5T_B$. The survival probability at each time step is obtained by projecting onto the *adiabatic* first excited state [5, 37]. Then the survival probability is averaged over the last 10% of the total integration time to estimate the asymptotic value of the survival probability. In the end, we average over 100 noise realisations and plot the standard deviation of the average survival probability as error bars.

The data for the noise-driven Wannier-Stark problem are generated in a similar way, by integrating the time-dependent Schrödinger equation for a 1D or 3D wavefunction. At $t = 0$, the system is prepared in the ground state of the bichromatic lattice potential superposed by a small harmonic trap potential (to keep the size of the initial wavefunction finite). At $t = 0$, the harmonic trap potential is disabled and replaced by the static force F . The survival probability in the ground band is measured by integration over the momentum distribution using appropriate boundaries (see [5, 34, 45, 50] for more details). While simulations for single-particle wave function were performed in one dimension, realistic results for the Gross-Pitaevskii equation can only be achieved using simulations in three dimensions (for the used algorithm, see [45]). For realistic values of the nonlinearity parameter, we used the values of the setup described in [46]: ^{87}Rb atoms in an optical lattice ($d_l = 426\text{nm}$) that are initially loaded into a cigar-shaped, quasi-one-dimensional optical trap, with 250Hz radial and 20Hz longitudinal confinement.

Appendix B. Unit conversion

Table B1: Summary of the new unit system. The table gives relations between our set of dimensionless units, SI-units and a set of common experimental units [5, 29, 30]. Here, M is the mass of the atoms in the BEC and k_L is the wavelength of the laser light used to generate the optical lattice. E_{rec} sets the characteristic energy scale of the system.

	Energy	Momentum	
1 photon exchange	$E_{\text{rec}} = \frac{\hbar^2 k_L^2}{2M}$	$p_{\text{rec}} = \hbar k_L$	
	SI-units	dimensionless	experimental
Energy	E_{SI}	$E = \frac{E_{\text{SI}}}{8E_{\text{rec}}}$	$E_{\text{exp}} = \frac{E_{\text{SI}}}{E_{\text{rec}}}$
Time	t_{SI}	$t = t_{\text{SI}} \frac{8E_{\text{rec}}}{\hbar}$	$t_{\text{exp}} = t_{\text{SI}}$
Space	x_{SI}	$x = 2x_{\text{SI}}k_L$	$x_{\text{exp}} = 2x_{\text{SI}}k_L$
Force	F_{SI}	$F_0 = \frac{F_{\text{SI}}}{16E_{\text{rec}}k_L}$	$F_{\text{exp}} = \frac{F_{\text{SI}}\pi}{E_{\text{rec}}k_L}$
Potential	V_{SI}	$V_0 = \frac{V_{\text{SI}}}{8E_{\text{rec}}}$	$V_{\text{exp}} = \frac{V_{\text{SI}}}{E_{\text{rec}}}$

References

- [1] Bason M G, Viteau M, Malossi N, Huillery P, Arimondo E, Ciampini D, Fazio R, Giovannetti V, Mannella R and Morsch O 2012/02 *Nature Physics* **8**(2) 147–152
- [2] Ferrari G, Poli N, Sorrentino F and Tino G M 2006 *Phys. Rev. Lett.* **97**(6) 060402
- [3] Holthaus M 2000 *Journ. of Opt. B: Quan. and Semicl. Opt.* **2** 589–604
- [4] Wilkinson S, Bharucha C, Madison K, Niu Q and Raizen M 1996 *Phys. Rev. Lett.* **76** 4512–4515
- [5] Tayebirad G, Zenesini A, Ciampini D, Mannella R, Morsch O, Arimondo E, Lörch N and Wimberger S 2010 *Phys. Rev. A* **82** 013633
- [6] Regensburger A, Bersch C, Miri M A, Onishchukov G, Christodoulides D N and Peschel U 2012 *Nature* **488** 167–171
- [7] Szameit A, Pertsch T, Nolte S, Tünnermann A, Peschel U and Lederer F 2007 *J. Opt. Soc. Am. B* **24** 2632–2639
- [8] Billy J, Josse V, Zuo Z, Bernard A, Hambrecht B, Lugan P, Clement D, Sanchez-Palencia L, Bouyer P and Aspect A 2008 *Nature* **453** 891–894
- [9] Jendrzejewski F, Bernard A, Muller K, Cheinet P, Josse V, Piraud M, Pezze L, Sanchez-Palencia L, Aspect A and Bouyer P 2012 *Nature Physics* **8** 398–403
- [10] Deissler B, Zaccanti M, Roati G, D’Errico C, Fattori M, Modugno M, Modugno G and Inguscio M 2010 *Nature Physics* **6** 354–358
- [11] Lucioni E, Deissler B, Tanzi L, Roati G, Zaccanti M, Modugno M, Larcher M, Dalfovo F, Inguscio M and Modugno G 2011 *Phys. Rev. Lett.* **106**(23) 230403
- [12] Roati G, D’Errico C, Fallani L, Fattori M, Fort C, Zaccanti M, Modugno G, Modugno M and Inguscio M 2008 *Nature* **453** 895–898
- [13] Modugno G 2012 Diffusion in noise-driven optical lattices private communication
- [14] Dykman M, Luchinsky D, Mannella R, McClintock P, Stein N and Stocks N 1995 *Il Nuovo Cimento D* **17**(7) 661–683 10.1007/BF02451825
- [15] Moss F and McClintock P V E 1989 *Noise in Nonlinear Dynamical Systems* (Cambridge University Press)
- [16] Kayanuma Y 1984 *Journ. of the Phys. Soc. of Japan* **54** 2037–2046
- [17] Pokrovsky V and Sinitsyn N 2003 *Phys. Rev. B* **67** 1–11
- [18] Luchinsky D G and McClintock P V E 1997 *Nature* **389** 463–466
- [19] Bray A J and McKane A J 1989 *Phys. Rev. Lett.* **62**(5) 493–496
- [20] Maier R and Stein D 1996 *Journal of Statistical Physics* **83**(3) 291–357 10.1007/BF02183736

- [21] Dykman M I, Mannella R, McClintock P V E, Stein N D and Stocks N G 1993 *Phys. Rev. E* **47**(6) 3996–4009
- [22] Schimansky-Geier L and Zülicke C 1990 *Zeit. für Phys. B Condensed Matter* **79** 451–460
- [23] Dykman M I, McClintock P V E, Smelyanski V N, Stein N D and Stocks N G 1992 *Phys. Rev. Lett.* **68**(18) 2718–2721
- [24] Dykman M I, Luchinsky D G, McClintock P V E and Smelyanskiy V N 1996 *Phys. Rev. Lett.* **77**(26) 5229–5232
- [25] Luchinsky D G, Maier R S, Mannella R, McClintock P V E and Stein D L 1997 *Phys. Rev. Lett.* **79**(17) 3109–3112
- [26] Luchinsky D G, Maier R S, Mannella R, McClintock P V E and Stein D L 1999 *Phys. Rev. Lett.* **82**(9) 1806–1809
- [27] Soskin S, Sheka V, Linnik T and Mannella R 2001 *Phys. Rev. Lett.* **86** 166, 5–1669
- [28] Avron J E 1982 *Annals of Physics* **143** 33 – 53
- [29] Tayebirad G, Mannella R and Wimberger S 2011 *Phys. Rev. A* **84** 031605(R)
- [30] Zenesini A, Lignier H, Tayebirad G, Radogostowicz J, Ciampini D, Mannella R, Wimberger S, Morsch O and Arimondo E 2009 *Phys. Rev. Lett.* **103** 090403
- [31] Glück M, Kolovsky A and Korsch H 2002 *Physics Reports* **366** 103–182
- [32] Arimondo E and Wimberger S 2011 Tunneling of ultracold atoms in time-independent potentials *Dynamical Tunneling Theory and Experiment* ed Schlagheck P (CRC Press) chap 11, pp 257–287
- [33] Tarallo M G, Alberti A, Poli N, Chiofalo M L, Wang F Y and Tino G M 2012 *Phys. Rev. A* **86**(3) 033615
- [34] Lörch N, Pepe F V, Lignier H, Ciampini D, Mannella R, Morsch O, Arimondo E, Facchi P, Florio G, Pascazio S and Wimberger S 2012 *Phys. Rev. A* **85**(5) 053602
- [35] Mannella R 2002 *International Journal of Modern Physics C* **13** 1177–1194 and references therein
- [36] Gardiner C 2004 *Handbook of Stochastic Methods* 3rd ed (Springer-Verlag Heidelberg)
- [37] Kraft M 2012 *Noise effects on Landau-Zener transitions of Bose-Einstein Condensates* MSci Thesis University of Heidelberg and Imperial College London
- [38] Lörch N 2010 *A study of open quantum systems* Diploma thesis University of Heidelberg
- [39] Zener C 1932 *Proc. of the Roy. Soc. London A* **137** 696–702
- [40] Landau L 1932 *Physics of the Soviet Union* **2** 46–51
- [41] Stückelberg E 1932 *Helvet. Phys. Acta* **5** 369–422
- [42] Majorana E 1932 *Nuovo Cimento* **2** 43–50
- [43] Vitanov N and Garraway B 1996 *Phys. Rev. A* **53** 4288–4304
- [44] Vitanov N 1999 *Phys. Rev. A* **59** 988–994
- [45] Burkhardt S 2012 *Noise assisted Interband Transitions in the Wannier-Stark Problem* Diploma thesis University of Heidelberg
- [46] Sias C, Zenesini A, Lignier H, Wimberger S, Ciampini D, Morsch O and Arimondo E 2007 *Phys. Rev. Lett.* **98**(12) 120403
- [47] Wimberger S, Mannella R, Morsch O, Arimondo E, Kolovsky A R and Buchleitner A 2005 *Phys. Rev. A* **72**(6) 063610
- [48] Dekorsy T, Bartels A, Kurz H, Ghosh A, Jönsson L, Wilkins J, Köhler K, Hey R and Ploog K 2000 *Physica E: Low-dimensional Systems and Nanostructures* **7** 279 – 284
- [49] Leo K 1998 *Semiconductor Science and Technology* **13** 249
- [50] Tayebirad G 2011 *Engineering the Landau-Zener Tunneling of Ultracold Atoms in Tilted Potentials* Ph.D. thesis University of Heidelberg